DOI:
10.1016/j.eurpolymj.2018.04.015

Document Version
Peer reviewed version

Accepted Manuscript

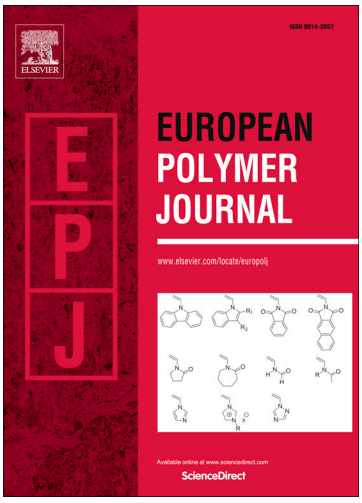

Green synthetic routes to alginate-graphene oxide composite hydrogels with enhanced physical properties for bioengineering applications

Ángel Serrano-Aroca, Lilis Iskandar, Sanjukta Deb

PII: S0014-3057(18)30476-2
DOI: https://doi.org/10.1016/j.eurpolymj.2018.04.015
Reference: EPJ 8371

To appear in: *European Polymer Journal*

Received Date: 9 March 2018
Accepted Date: 11 April 2018

Please cite this article as: Serrano-Aroca, A., Iskandar, L., Deb, S., Green synthetic routes to alginate-graphene oxide composite hydrogels with enhanced physical properties for bioengineering applications, *European Polymer Journal* (2018), doi: https://doi.org/10.1016/j.eurpolymj.2018.04.015

Green synthetic routes to alginate-graphene oxide composite hydrogels with enhanced physical properties for bioengineering applications

Ángel Serrano-Aroca[1,*], Lilis Iskandar[2], Sanjukta Deb[2,*]

[1] Facultad de Veterinaria y Ciencias Experimentales, Universidad Católica de Valencia San Vicente Mártir, C/Guillem de Castro 94, 46001 Valencia, Spain.

[2] Division of Tissue Engineering & Biophotonics, King's College London, Dental Institute, London, Floor 17, Tower Wing, Guy's Hospital, London SE1 9RT, UK.

Email L. I.: lilis.iskandar@kcl.ac.uk

*Corresponding authors. Email: angel.serrano@ucv.es (Ángel Serrano-Aroca). Email: sanjukta.deb@kcl.ac.uk (Sanjukta Deb)

Abstract

Hydrogels are being increasingly utilized in bioengineering applications such as tissue engineering because they are able to mimic the specific environments of extracellular matrices and in bioprocess engineering to immobilise cells or enzymes as catalysts. Alginate hydrogels holds great promise in these industrial fields, however, they are mechanically weak, which necessitates composites or hybrid materials to modulate their properties without compromising other important physical properties such as water diffusion, which plays a very important role in the nutrient exchange with the surrounding environment. Efforts to fabricate alginate-based composites reinforced with graphene oxide (GO) have been reported, however there are challenges in enhancing mechanical and other physical properties at the same time, and facile large-scale production. In this study, we report two novel green engineering routes of fabricating calcium alginate-GO hydrogels and compare with the conventional procedure to synthesise alginates via bulk chelation with calcium chloride. The two new methods yielded nanocomposites with significant increases in tensile modulus (up to 2.5 times) and markedly faster water diffusion (> 4 times) in comparison to the conventional method. In addition, wettability and thermal properties were also enhanced, which was attributed to the novel structure organisation.

Keywords: graphene oxide, calcium alginate, composite hydrogels, biomedicine, bioprocesses, bioengineering.

1. Introduction

Tissue engineering approaches have undoubtedly become a promising strategy for repairing damaged or diseased tissue[1]. Scaffold based engineering of tissues primarily require the scaffold to allow the diffusion of nutrients and metabolites whilst providing structural support[2]. The biophysical properties of alginate hydrogels, ability to crosslink them with divalent ions, tunable mechanical properties and thereby create an environment favourable to cell proliferation and differentiation make them attractive for biomedical applications. A promising approach to obtain hydrogels with superior properties is by integrating carbon-based nanomaterials within their network structure, enabling a combination advantageous for tissue engineering applications[3].

Alginate is a biopolymer produced from renewable sources such as brown algae[4] or microorganisms[5]. Alginates are composed of D-mannuronic (M) and L-guluronic (G) acid residues, with M and G present in varying proportions and sequences depending on the alginic acid source. The gelation process starts when calcium cations interact with blocks of G residues to form the *egg-box model* buckled structure[6]. The ability of alginates to form insoluble gels on reacting with divalent metal cations, specifically calcium ions, renders it extremely useful for encapsulation, pharmaceuticals and other biological applications[7,8]. The conventional method of forming calcium alginate films involve preparing sodium alginate films via air drying, which are subsequently immersed in concentrated $CaCl_2$ aqueous solution to enable crosslinking[9]. However, other synthetic routes have been reported such as directly mixing different amounts of calcium chloride (0.04, 0.08 and 0.12g $CaCl_2$/4 g alginate) into sodium alginate film-forming solutions that display different physical and mechanical properties[10]. One of the main disadvantages of a direct mixing of these two components is the heterogeneity

of the resulting gel networks due to the very fast and irreversible crosslinking reaction [7].

Alginates are very promising polysaccharides with many potential applications in biotechnology[1,11], water treatment[12], plastic packaging materials[13] due to its non-toxicity, biodegradability, biocompatibility, ease of gelation and relative economic cost in comparison with other polymers. However, this polymer like most hydrogels exhibits weak mechanical properties, especially in the hydrated state, which restrict their number of industrial applications. Thus, much effort is being directed in the reinforcement of polymers with improvements being reported through several methods: block copolymerisation with some hydrophobic domains[14,15], increase of crosslinking density[16–18], interpenetrating polymer networks (IPNs)[19], fiber filling[20], sol-gel process[21], plasma-polymerisation grafting onto a porous hydrophobic substrate[22–24] and by incorporation of nanomaterials such as graphene oxide (GO)[25–29].

GO is a fascinating two dimensional nanomaterial with a large surface area decorated with a number of functional groups (hydroxyls, carbonyls and epoxy groups) located at the edges and basal planes, which allow them to yield stable suspensions in distilled water. Graphene oxide exhibits excellent physical properties, biocompatibility and nontoxicity[30] that have led to immense promising applications in environmental science, optics, electronics, energy conversion and in biomedicine specially for drug delivery and drug binding effectors for hydrogel functionalization[31,32]. In addition, the antibacterial activity of GO in nanocomposites[33,34] widens the scope of this very promising nanofiller in the biomedical and bioprocess industries where contamination is difficult to avoid. Hence, alginate-graphene oxide composites have been fabricated in various forms, such as films of sodium alginate-GO [35] and fibers of calcium alginate-

GO [36] by wet spinning to enhance thermal and mechanical properties. GO nanosheets have been reported as a reinforcing filler in ternary composites with sodium alginate/polyacrylamide nanocomposite and calcium-alginate-pectinate-cellulose acetophthalate gelispheres with enhanced mechanical properties to widen the scope in drug delivery applications[37,38]. Furthermore, calcium alginate-graphene oxide composite films prepared by the direct mixing method have recently exhibited a very significant improvement of compressive modulus and water diffusion with a minuscule amount of GO when a high amount of calcium chloride is added to the reactive mixture [25]. However, as already mention, this synthetic route produces very heterogeneous gel networks [7] and engineering routes, based on the conventional method [9], for yielding more homogeneous gels with optimum properties have not yet been explored. Herein, we report the formation of abundant three-dimensional cross linked networks by coordination chemistry, similar to processes used in cross-linking of carbon nanotubes (CNTs)[39], chemically modified graphene (CMG) with CNTs[4] and GO[40,41]. It has been demonstrated that this crosslinking of GO nanosheets with divalent cations of calcium can enhance very significantly the mechanical[42] and water diffusion[25] properties of calcium alginate. This improvement of water diffusion is very important to improve cell survival in biomedical fields such as tissue engineering[2] and increase productivity[11] in bioprocess engineering through enhancement of mass transfer in immobilised cells or enzymes (biocatalysts)[4]. Thus, in this study, crosslinking between GO nanosheets was performed before (synthetic route 2: S2) and during gelation (synthetic route 3: S3) by coordination with divalent atoms of calcium in the alginate polymer matrix. GO/calcium alginate nanocomposites were also synthesised by the conventional synthetic route wherein sodium alginate is soaked in a concentrated

aqueous solution of calcium chloride (synthetic route 1; S1) to enable direct comparison of properties.

2. Experimental

2.1. Materials

Sodium alginate, calcium chloride (≥ 93.0%, Sigma-A1112, 12-80 kDa) and graphene oxide were purchased from Sigma-Aldrich and utilized without further purification.

2.2. Synthetic routes

Three synthetic routes were followed to synthesize the calcium alginate-graphene oxide hydrogels. The concentration of graphene oxide was maintained at 1% by weight with respect to the mass of sodium alginate. These graphene oxide-calcium alginate composite hydrogels are hereafter referred to as R1, R2 and R3 according to the synthetic routes followed using method S1, S2 and S3 respectively

2.2.1. Synthetic route 1(S1)

A sodium alginate/graphene oxide (99/1) mixture was prepared with 1.5g of sodium alginate and 0.0151g of GO dissolved in 60 ml of distilled water under continuous magnetic stirring. This mixture was then poured into Petri dishes to allow the water to evaporate slowly at room temperature (24±1°C) for 24 hours. After that, the formed pre-sample was soaked into a 10% (w/v in g/mL) calcium chloride aqueous solution for two hours, thereafter rinsed with distilled water and dried at 60°C in vacuum.

2.2.2. Synthetic route 2 (S2)

In this chemical procedure, a pre-sample of sodium alginate with 6 wt. % of calcium chloride and GO was prepared by solvent casting. This percentage of $CaCl_2$ was determined empirically by trial and error to achieve an addition of calcium atoms large enough to produce crosslinking between the GO nanosheets and small enough to keep the final mixture in a sol state to enable a slow gelation process during the solvent casting process. Thus, three solutions were prepared under continuous magnetic stirring at room temperature (24±1°C): 1.5g of sodium alginate dissolved in 50 ml of distilled water (solution 1), 0.0151g of GO in 10 ml of distilled water (solution 2) and 0.0957 g of $CaCl_2$ in 10 ml of water (solution 3). Subsequently solution 2 and 3 were mixed and magnetically stirred for 1 hour to initiate crosslinking of GO before this mixture was added to solution 1 and further magnetically stirred for 10 minutes This mixture was then poured into Petri dishes to allow the water to evaporate slowly at room temperature for 24 hours. Finally, the pre-samples were immersed in a bath of 10% (w/v in g/mL) calcium chloride aqueous solution for two hours, rinsed with distilled water and dried at 60°C in vacuum.

2.2.3. Synthetic route 3 (S3)

The method in this route was similar to S2, however the GO crosslinking was carried out simultaneously with the gelation, hence solution 1 and 2 were mixed under continuous magnetic stirring till homogenous and then solution 3 was added with a further magnetic stirring for 10 minutes.

2.3. Characterisation

2.3.1. Microscopy

The morphology of the GO nanosheets was examined under field emission scanning electron microscopy (FESEM) at a magnification of 100000x using a Zeiss Ultra 55 Model microscope operating at 2 kV.

GO nanosheets before and after reacting with calcium chloride were observed by high resolution transmission electron microscopy (HR-TEM) with scanning transmission electron microscopy (STEM) dark field imaging at a magnification of 300000 with a JEOL-TEM 2100F 200 kV microscope. HRTEM sample preparation consisted of dispersing the samples with dichloromethane in an ultrasonic bath for ten minutes and subsequent drying at ambient temperature (24±1ºC).

The GO/calcium alginate nanocomposites were observed on a TSM Tandem scanning confocal microscope (TSM) (Noran Instruments, USA) equipped with a Motorized Lab Jack (Thorlabs Ltd, UK) in conjunction with an EMCCD camera iXon 885 EM-CCD, 40X/0.55NA lenses and iQ capture software (Andor Technology, UK).

2.3.2. Water sorption studies

Water content (w) as g water/g dry sample was determined as a function of time by gravimetric measurements at specific time intervals at room temperature (24±1ºC). Thus, the equilibrium water content (w_{eq}) and the water diffusion coefficients of the composite samples were calculated. The experiments were performed in triplicate to analyse the reproducibility of the results (mean and standard deviation).

2.3.3. Tensile testing

Tensile testing was performed on test specimens (2 cm in length x 5 mm in width) using a universal testing machine (Instron, Model 5569A, USA) at a crosshead speed of 2 mm/min. The nanocomposites were hydrated in distilled water for two hours to ensure

water sorption equilibrium (w_{eq}) at ambient temperature (24±1°C) and kept moist during the testing. Six specimens of each type of nanocomposite were tested. Their dimensions in hydrated state were measured using a digital electronic calliper.

2.3.4. Wettability measurements

Contact angles (CA) and surface free energy (SFE) were measured by the sessile drop method placing ten 5 μl droplets on rectangular bar specimens at ambient temperature (24±1°C). Two liquids (water and methylene iodide) were used with opposite polarity and known total surface free energy (Y_l=72,8 mN/m^2 and Y_l=51,8 mN/m^2 respectively). Contact angles were determined from the photographs taken with a high-resolution digital camera right after the drops are located on the solid samples. ImageJ software was employed to process the profile of the drops and thus calculate the contact angles.

2.3.5. Differential Scanning Calorimetry

The thermal properties of 5-10 mg vacuum dried composite samples sealed in aluminium pans were studied with a Jade series differential scanning calorimeter (DSC). A Perkin Elmer Jade series software was utilized to process raw data and all the scans were performed with reference pan calibrated using Indium^{49} under a Nitrogen^{7} atmosphere (20 ml/min). The DSC thermal program consisted of subjecting the composite samples to a cooling scan from ambient temperature down to -30°C, followed by a heating scan from that low temperature up to 300°C at 10°C/min. These scans were carried out twice for each composite to confirm their reproducibility.

2.3.6. Fourier Transform Infrared Spectroscopy

Fourier transform infrared (FTIR) transmission spectroscopy from 650 to 4000 cm^{-1} was performed on a Perkin Elmer Spectrum One Fourier Transforms Infrared spectrometer.

3. Results & discussion

The graphene oxide employed in this study consisted of nanosheets of 100-200 nm in length (see Figure 1a), which can react with divalent calcium cations to form irregular micrometre length tubes of GO by coordination chemistry (Figure 1b-d).

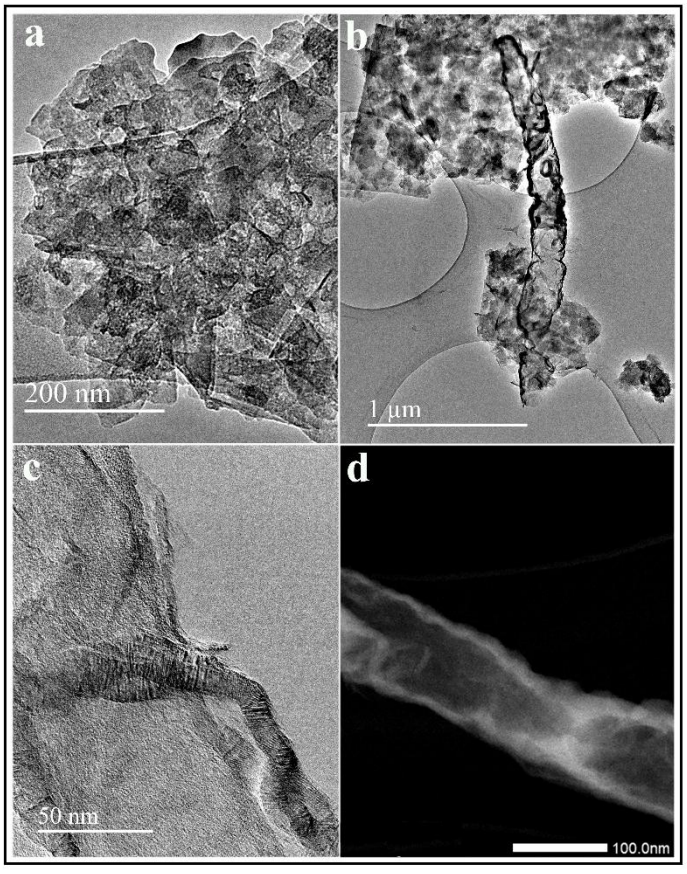

Figure 1. High-resolution transmission electron micrographs of GO before (a) and after crosslinking with Ca^{2+} cations at two magnifications (b&c). STEM dark field image of GO crosslinked with Ca^{2+} cations (d).

These folded 3D crosslinked GO networks were produced by dispersing the GO powder in distilled water and subsequent mixing with a 10 w/v% calcium chloride aqueous solution with continuous magnetic stirring at 24±1°C following the same procedure described in [26]. It is of notice that some crosslinking without folding of GO nanocheets also occurs (see Figure 1b).

The graphene oxide powder utilised in this study showed a structure of nanosheets stacked together by van der Waals forces and π-π interactions by FESEM (see Figure 2a). This chemical attraction of GO can explain the biphasic morphology of the R1 nanocomposite (Figure 2b). Thus, this confocal microscopy image shows a biphasic structure composed of GO (dark phase) and calcium alginate (clear phase) due to GO nanosheets stack together during this chemical route without hardly GO crosslinking. However, the nanocomposite R2 (Figure 2c) was derived from pre-crosslinking of the graphene oxide sheets in presence of an aqueous solution of calcium chloride, which led to the formation of crosslinked GO networks (Figure 1b-d), whilst in the R3 material (Figure 2d) the crosslinking with the divalent cations was carried during gelation.

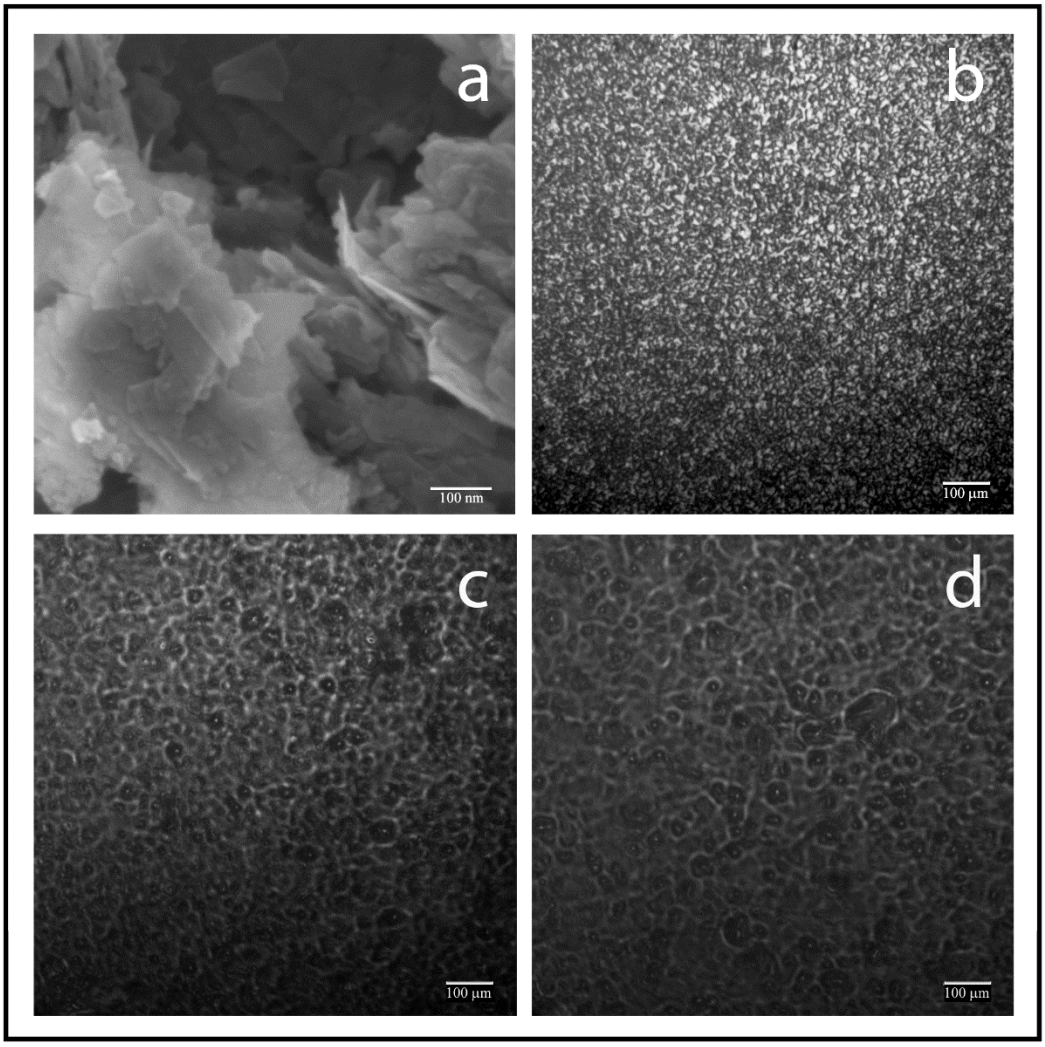

Figure 2. FESEM (100000X) of graphene nanosheets (a) and confocal microscopy of nanocomposites R1 (b), R2 (c) and R3 (d). The GO is the dark phase and the calcium alginate matrix is the clear phase.

In the R2 and R3 nanocomposites, crosslinking occurs between the GO nanosheets, GO with alginate chains and between alginate chains by coordination via divalent calcium atoms (see Figure 3). Irregular folding of the crosslinked GO nanosheets (Figure 1b-d) is possible due to the coordination reactions between the calcium cations and the oxygen-containing groups located at the basal planes and at the edges of GO.

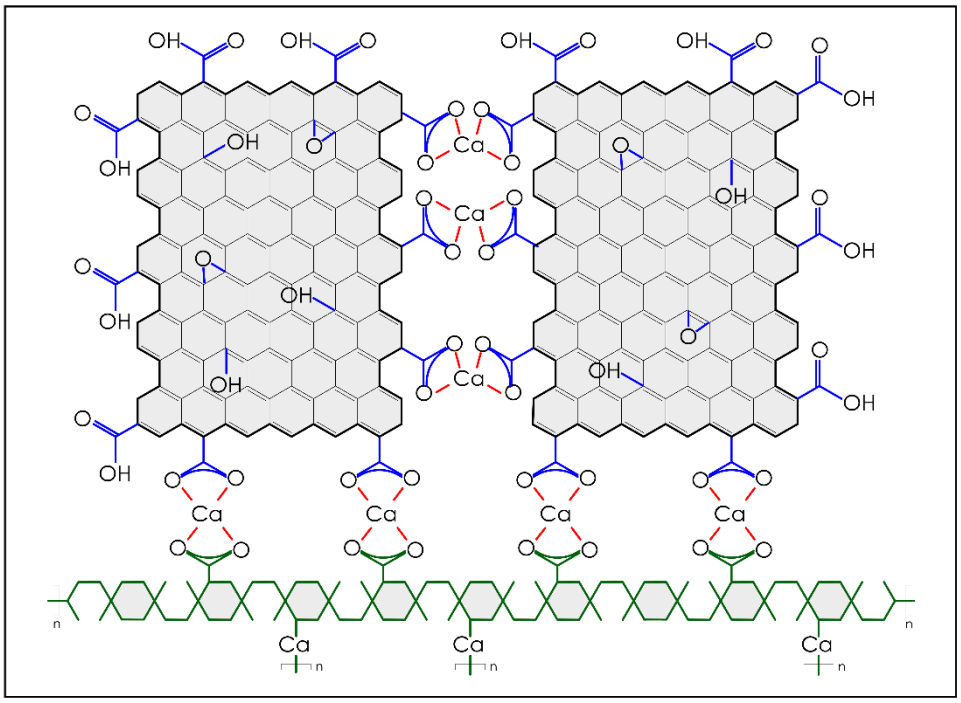

Figure 3. Crosslinking of between graphene oxide nanosheets, between graphene oxide and alginate chains and between alginate chains.

Thus, the micrometer-size domains of the continuous crosslinked GO aggregates surrounded by calcium alginate chains can be observed clearly in [figure 2(c) and (d)] in contrast to R1 [figure 2(b)]. However, since in R3, GO crosslinking occurs during the gelation process, there are many more available sites for crosslinking between GO nanosheets and alginate chains, rendering this nanocomposite more mechanically resistant than R2 (figure 5).

The equilibrium water content of the nanocomposite hydrogels are shown in Table 1. The typical uptake as a function of $t^{1/2}$ in Figure 4, which showed that R3 had higher values with respect to R2 and R1. The diffusion coefficients of liquid water in these nanocomposite systems were calculated according to the Fick's law assuming that Equation (1) holds for $\Delta m_{1,t}/\Delta m_{1,\infty} < 0.5$

$$\frac{\Delta m_{1,t}}{\Delta m_{1,\infty}} \approx 4\left(\frac{Dt}{\pi \cdot l^2}\right)^{\frac{1}{2}} \quad (1)$$

where $\Delta m_{1,t}$ and $\Delta m_{1,\infty}$ are the weight increments at time t and at equilibrium respectively, l is the nanocomposite thickness and D the diffusion coefficient. The equilibrium water contents were utilised to determine $\Delta m_{1,\infty}$ in the $\Delta m_{1,t}/\Delta m_{1,\infty}$ vs. $t^{1/2}/l$ plot. Figure 3 shows that all the sorption curves do not follow a Fickian diffusion profile[43]. Similar results were determined in earlier studies performed with calcium and barium alginate films in liquid water [44] and alginate-(reduced)graphene oxide nanocomposites[45]. The apparent water diffusion coefficient was calculated with Equation (1) adjusted in the linear range of all these plots during the early period of the uptake to determine the liquid water diffusion capacity of these nanocomposite hydrogels.

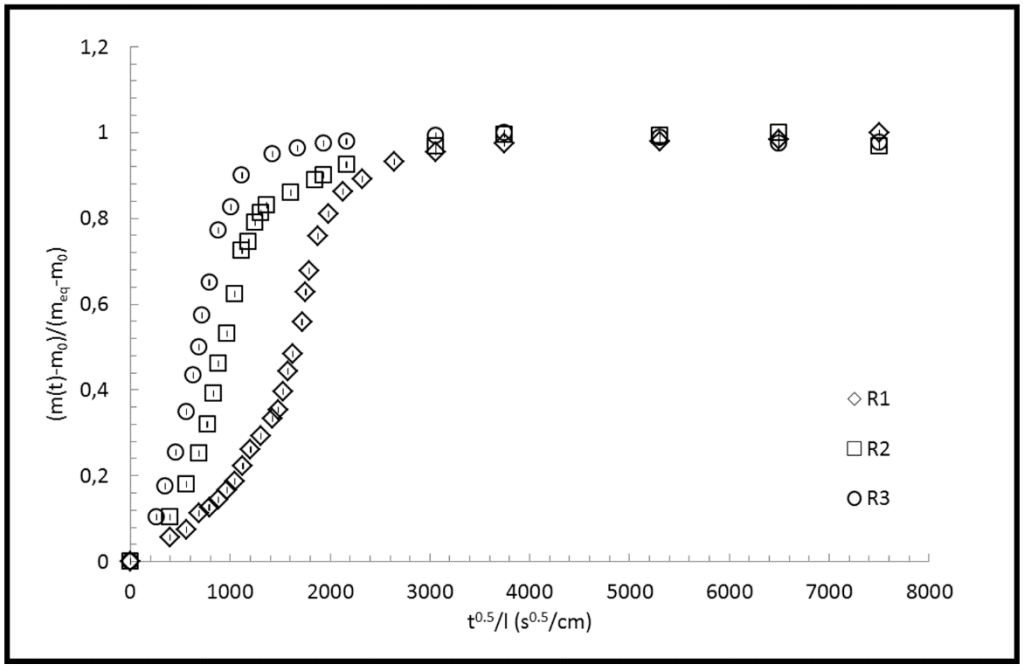

Figure 4. Example of plots used to calculate the apparent diffusion coefficient of liquid water in R1, R2 and R3 composite hydrogels adjusting Fick's law in the linear range of these graphs in early time intervals.

Nanocomposite	w_{eq} ($m_{water}/m_{dry\ sample}$)	$D(cm^2/s)\cdot10^7$
R1	0.58±0.02	0.33±0.16
R2	0.58±0.15	1.48±0.19
R3	0.71±0.04	1.37±0.19

Table 1. Equilibrium water contents (w_{eq}) and apparent diffusion coefficient (D), (assuming Fick's law is obeyed). Data are plotted as mean±SD.

The apparent diffusion coefficient of liquid water in R2 and R3 was markedly higher (> 4 times) in comparison to the conventional method (R1) (see Figure 4 and Table 1), which can be explained due to calcium cations are able to crosslink both alginate and graphene oxide nanosheets to form cross-linked GO networks inside the hydrogels of calcium alginate [25], which must yield longer and larger porous nanochannels, assuming that there is crosslinking between GO nanosheets at the basal planes and at the edges in comparison to R1 facilitating easier water transport within the nanocomposite polymer network. This increase in water diffusion produced by the addition of graphene oxide related well with the recently explained fast diffusion of water on graphene [46]. Besides, it has been reported that liquid water can afford an ultrafast permeation through graphene-based nanochannels with a faster diffusion coefficient 4-5 times greater than in the bulk case[47] and ultrafast transport of water molecules through pores composed of hydrophobic graphitic nanochannels in membranes composed of aligned carbon nanotubes[48,49] and GO membranes[50,51].

The mechanical behaviour of the hydrated nanocomposite films, after immersion in liquid water to equilibrium water content w_{eq} (see Table 1), was analysed by tensile tests and Figure 5 shows typical stress-strain curves.

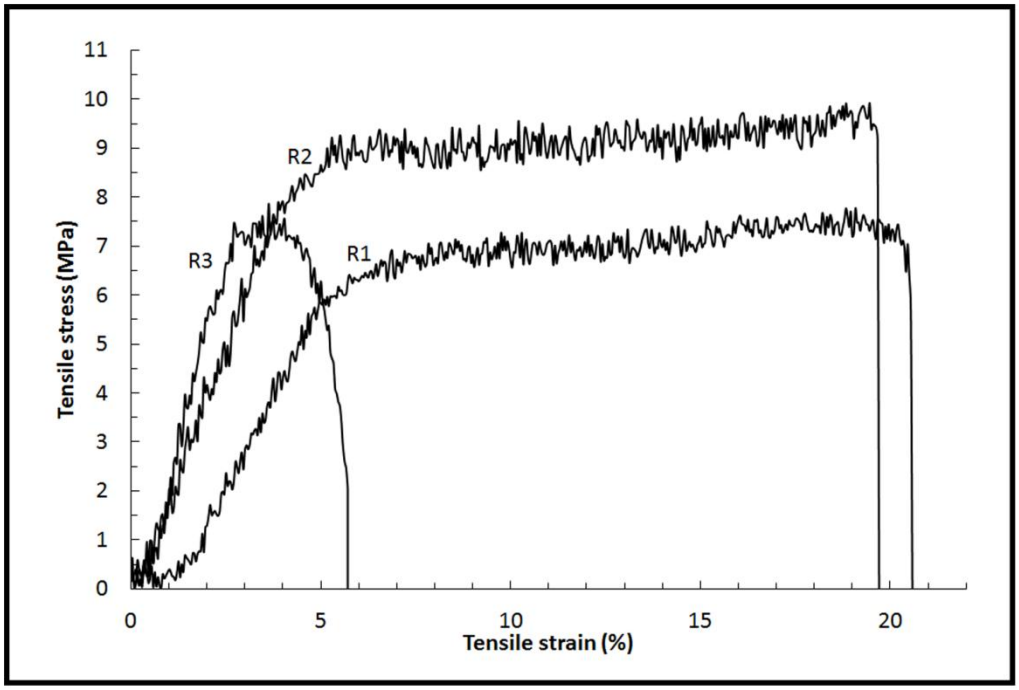

Figure 5. Example of typical tensile stress versus strain curves of the hydrated nanocomposite films of R1, R2 and R3.

The tensile strength and modulus as a function of the synthetic route are summarized in Table 2, which demonstrates a significant increase in the tensile strength and modulus of the R2 and R3 composites. However, the modulus of R3 was statistically significantly higher in comparison to both R1 and R2. The tensile strength and tensile modulus were calculated and differences were analysed by one-way ANOVA and Tukey's post hoc analysis at significance level of $p < 0.01$.

Ca-alginate-GO composite	Tensile strength (MPa)±SD	Tensile modulus (GPa) ±SD
R1	6.43±0.47	0.28±0.04
R2	8.21±0.60	0.46±0.05
R3	8.98±0.35	0.70±0.07

Table 2. Tensile strength and modulus of hydrated composite films R1, R2&R3 synthesised by the three different routes (n=6, SD: standard deviation). Data are plotted as mean±SD. Differences were statistically significant with respect to R1 ($p<0.01$).

Although, earlier reports also confirm a reinforcement of sodium alginate films (dry films) with a relatively low amount (1 wt. %) of graphene oxide exhibiting 1.6 and 1.15 times increases in the tensile modulus and stress values respectively. Additionally, higher amounts of GO (from 2.5 to 6 wt. %) caused a significant increase in tensile strength and Young's modulus of 1.38 and 3 times respectively[35]. However, these nanocomposites are not suitable for applications in contact with water without crosslinking. Hydrated calcium alginate prepared by the conventional method of immersing films in the coagulation bath of $CaCl_2$ have been shown to exhibit higher tensile modulus and strength of 5.4±0.7 and 2.0±1.5 MPa[44], which is much lower than any nanocomposite synthesised in this study, however they may be attributed to the differences in the molecular weight and the G/M composition of sodium alginate. The tensile strength and modulus of the films prepared in this study via the different routes clearly demonstrate that the values are significantly greater for the R2 & R3 films and more so for the modulus of the R3 films. The improvement of mechanical properties of the sodium alginate/GO films is mainly attributed to compatibility, alignment and specific interactions of alginate OH groups with GO oxygenated functional groups rather than to alginate crystallinity modification due to hydrogen bonding and high interfacial adhesion between GO and the sodium alginate polymer matrix[35]. However, in the calcium alginate-GO composites synthesised in this work, the enhancement of mechanical properties must also be attributed to the complexation reaction that occurs between GO and the divalent calcium atoms, which render calcium alginate nanocomposites much more reinforced because of the continuous cross-linked GO networks distributed around their calcium alginate polymer structure with additional crosslinking between calcium alginate chains and cross-linked GO networks, whilst the degree of crosslinking achieved is dependent on the synthetic route.

In addition, other physical properties measured in this studied such as wettability and glass transition temperature also increased significantly demonstrating the importance of these two new synthetic routes (see Table 3). The surface free energy (Y_s) of the three samples was determined by the Fowkes'[52] and Owens'[53] method with the following equations.

$$Y_s = Y_s^d + Y_s^p \quad (2)$$

$$(1 + cos\theta)Y_l/2 = (Y_s^d Y_l^d)^{1/2} + (Y_s^p Y_l^p)^{1/2} \quad (3)$$

where Y_s^d, Y_s^p, Y_l^d and Y_l^p are the dispersive and polar components of Y_s of solid and liquid, respectively. These polar and dispersive values for the two tested liquids (water and methylene iodide) were taken from the literature[54]. These results show that the contact angle values decreased in both new chemical routes in comparison with the conventional method, which resulted in a significant increase of the calculated surface free energy, rendering the surfaces of these nanocomposites R2 and R3 more hydrophilic. Remarkably the hydrophilicity achieved by performing the GO crosslinking prior to gelation is considerably much higher and render this route 2 highly suitable to synthesise GO/calcium alginate nanocomposites with enhanced hydrophilicity.

Nanocomposite	$\theta(H_2O)$	$\theta(CH_2I_2)$	Y_s(mN/m)	Y_s^d(mN/m)	Y_s^p(mN/m)	$T_g(°C)$
R1	50.8±2.6	39.8±2.3	57.8±1.2	40.8±1.0	17.3±1.8	69.74
R2	40.6±2.9	37.8±2.9	64.1±1.8	41.6±1.4	22.6±1.7	74.67
R3	47.1±2.6	34.5±2.4	61.4±1.4	43.1±1.1	18.3±1.6	77,02

Table 3. Water ($\theta(H_2O)$) and Methylene iodide ($\theta(CH_2I_2)$) contact angle, solid surface free energy (Y_s) with their dispersive (Y_s^d) and polar(Y_s^p) components, and glass transition temperature (T_g) for the composites synthesised by route 1, 2 and 3. Data are plotted as mean±SD.

Although there was clearly an increase in the apparent diffusion coefficients and hydrophilicity of the films obtained via Routes 1 and 2, the glass transition of the nanocomposites increased from the first to the third synthetic route due to the increasing degree of crosslinking between the GO sheets, which increasingly restrict conformational movements of the calcium alginate polymeric macromolecules. The DSC thermograms showed a significant enhancement of thermal properties for R2 and R3 samples as compared to R1. Thus, the R1 composite sample exhibited a more heterogeneous behaviour with more crystallisation peaks starting at lower temperature than R2 and R3 (Figure 6).

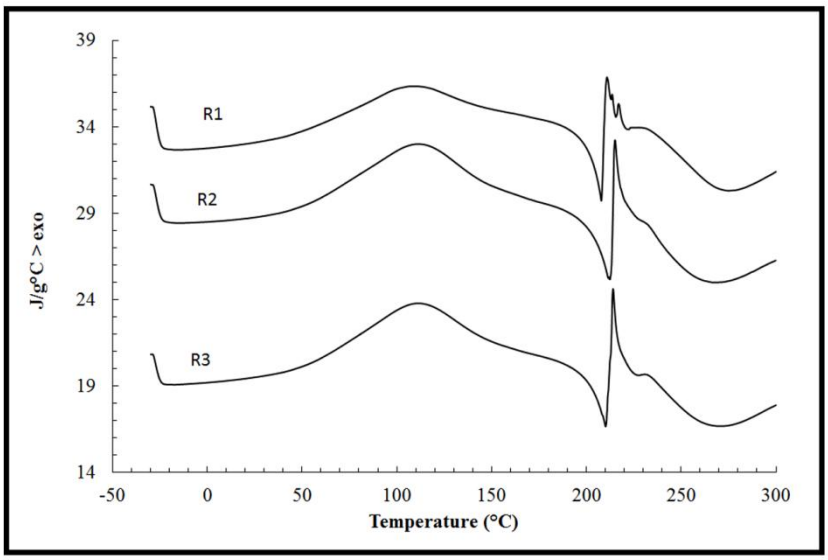

Figure 6. DSC thermograms of the calcium alginate nanocomposites (R1, R2 and R3) at a heating rate of 10ºC/min.

The FTIR spectra of the three composite hydrogels are shown in Figure 7 with a broad peak around 3250 cm^{-1} attributed to the hydroxyl group stretching vibration, two

narrower peaks at 1600 cm^{-1} and 1414 cm^{-1} corresponding to symmetric and asymmetric COO- stretching vibration, and a strong peak around 1030 cm^{-1} due to the C-O-C stretching vibration[35]. The FTIR spectra of R2 and R3 shows a stronger and broader band at 1030 cm^{-1} with respect to the intensity of the band appearing at 1600 cm^{-1} than in R1. The shoulder peak around 1087 cm^{-1} corresponds to the C-O stretching vibration of sodium alginate[55]. These stronger peaks in the fingerprint region at 1000-1260 cm^{-1} due to the C-O-C and C-O stretch are typically observed when carboxylic acid groups coordinate with divalent metal ions[56], which can potentially lead to cross-links between the GO nanosheets.

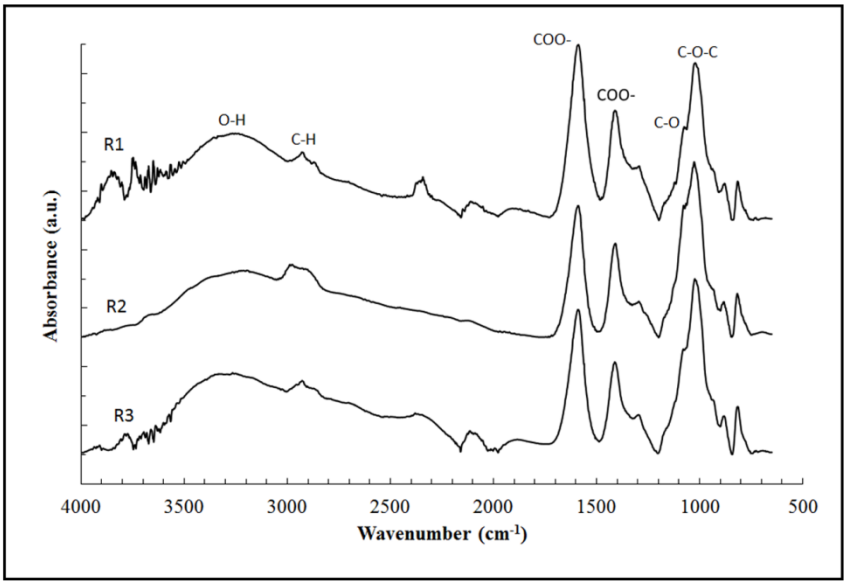

Figure 7. FTIR spectra of the GO/calcium alginate nanocomposites (R1, R2 and R3).

4. Conclusion

Alginate composite hydrogels were synthesised with calcium chloride as crosslinking agent and 1 wt. % of graphene oxide following two different synthetic methods and compared with the conventional synthetic procedure of dropping sodium alginate into an aqueous coagulation bath of calcium chloride. These chemical procedures differ from

each other on the steps followed to achieve different degrees of crosslinking between the GO nanosheets by metal coordination chemistry and distribution in the polymer matrix. Thus, significant increases in liquid water diffusion (> 4 times) and tensile properties (up to almost 2.5 times higher) can be achieved by the new synthetic routes in comparison with the conventional one, which make them extremely suited for bioengineering applications such as tissue engineering, bioprocess engineering, drug carriers and other industrial applications with higher mechanical and liquid water diffusion requirements. In addition, the surface tension, glass transition temperature and equilibrium water content of these new composite hydrogels also improved significantly demonstrating the importance of these green synthetic procedures. The scope is very broad as this clean and facile technology exhibits affordable large-scale production of three dimensional calcium alginate-GO composite networks with higher crosslinking using distilled water as solvent without consuming thermal or sonic energy, thus accomplishing the goals of green chemistry and sustainable technologies.

Acknowledgments

The authors would like to acknowledge the Universidad Católica de Valencia San Vicente Mártir and the Ministry of Economy, Industry and Competitiveness for the financial support of this work through the 2018-231-001UCV and MAT2015-69315-C3-1-R grants respectively, and the Government of Indonesia.

References

[1] B.D. Ratner, A.S. Hoffman, F.J. Schoen, J.E. Lemons, Biomaterials Science: An Introduction to Materials in Medicine, Academic Press, Canada, 2012.

[2] C. Van Blitterswijk, J. De Boer, Tissue engineering, Academic Press, 2014.

[3] M. Mehrali, A. Thakur, C.P. Pennisi, S. Talebian, A. Arpanaei, M. Nikkhah, A. Dolatshahi-Pirouz, Nanoreinforced Hydrogels for Tissue Engineering: Biomaterials that are Compatible with Load-Bearing and Electroactive Tissues, Adv. Mater. 29 (2017) 1603612. doi:10.1002/adma.201603612.

[4] D.L. Kaplan, ed., Biopolymers from Renewable Resources, Springer Berlin Heidelberg, Berlin, Heidelberg, 1998.

[5] P. Vauchel, R. Kaas, A. Arhaliass, R. Baron, J. Legrand, A New Process for Extracting Alginates from Laminaria digitata: Reactive Extrusion, Food Bioprocess Technol. 1 (2008) 297–300.

[6] G.T. Grant, E.R. Morris, D.A. Rees, P.J.C. Smith, D. Thom, Biological interactions between polysaccharides and divalent cations: The egg-box model, FEBS Lett. 32 (1973) 195–198.

[7] K.I. Draget, Handbook of Hydrocolloids, Elsevier, 2009. doi:10.1533/9781845695873.807.

[8] T. Huq, C. Fraschini, A. Khan, B. Riedl, J. Bouchard, M. Lacroix, Alginate based nanocomposite for microencapsulation of probiotic: Effect of cellulose nanocrystal (CNC) and lecithin, Carbohydr. Polym. 168 (2017) 61–69. doi:10.1016/j.carbpol.2017.03.032.

[9] A.E. Pavlath, A. Voisin, G.H. Robertson, Pectin-based biodegradable water insoluble films, Macromol. Symp. 140 (1999) 107–113.

[10] J.W. Rhim, Physical and mechanical properties of water resistant sodium alginate

films, LWT - Food Sci. Technol. 37 (2004) 323–330.

[11] P.M. Doran, Bioprocess Engineering Principles, Academic Press, United Kingdom, 2013.

[12] K. Draget, G. Skjakbrak, O. Smidsrod, Alginic acid gels: the effect of alginate chemical composition and molecular weight, Carbohydr. Polym. 25 (1994) 31–38.

[13] E.M. Zactiti, T.G. Kieckbusch, Release of potassium sorbate from active films of sodium alginate crosslinked with calcium chloride, Packag. Technol. Sci. 22 (2009) 349–358.

[14] M. Pérez Olmedilla, N. Garcia-Giralt, M.M. Pradas, P.B. Ruiz, J.L. Gómez Ribelles, E.C. Palou, J.C.M. García, Response of human chondrocytes to a non-uniform distribution of hydrophilic domains on poly (ethyl acrylate-co-hydroxyethyl methacrylate) copolymers, Biomaterials. 27 (2006) 1003–1012.

[15] R. Brígido-Diego, M. Pérez-Olmedilla, Á. Serrano-Aroca, J.L. Gómez-Ribelles, M. Monleón-Pradas, G. Gallego-Ferrer, M. Salmerón-Sánchez, Acrylic scaffolds with interconnected spherical pores and controlled hydrophilicity for tissue engineering, J. Mater. Sci. Mater. Med. 40 (2005) 4881–4887. doi:10.1007/s10853-005-3885-4.

[16] M. Monleón-Pradas, J.L. Gómez-Ribelles, Á. Serrano-Aroca, G. Gallego-Ferrer, J. Suay-Antón, P. Pissis, Interaction between water and polymer chains in poly(hydroxyethyl acrylate) hydrogels, Colloid Polym. Sci. 279 (2001) 323–330.

[17] Á. Serrano-Aroca, M. Monleón-Pradas, J.L. Gómez-Ribelles, Effect of crosslinking on porous poly(methyl methacrylate) produced by phase separation,

Colloid Polym. Sci. 286 (2008) 209–216.

[18] Á. Serrano-Aroca, M. Llorens-Gámez, Dynamic mechanical analysis and water vapour sorption of highly porous poly(methyl methacrylate), Polymer (Guildf). 125 (2017) 58–65. doi:10.1016/j.polymer.2017.07.075.

[19] P. Li, X.-Q. Dou, C.-L. Feng, D. Zhang, Mechanical reinforcement of C2-phenyl-derived hydrogels for controlled cell adhesion, Soft Matter. 9 (2013) 3750–3757.

[20] A. Khoushabi, A. Schmocker, D.P. Pioletti, C. Moser, C. Schizas, J.A. Manson, P.E. Bourban, Photo-polymerization, swelling and mechanical properties of cellulose fibre reinforced poly(ethylene glycol) hydrogels, Compos. Sci. Technol. 119 (2015) 93–99.

[21] J.C. Rodríguez-Hernández, Á. Serrano-Aroca, J.L. Gómez-Ribelles, M. Monleón-Pradas, Three-dimensional nanocomposite scaffolds with ordered cylindrical orthogonal pores, J. Biomed. Mater. Res. - Part B Appl. Biomater. 84 (2008) 541–549.

[22] Á. Serrano-Aroca, M. Monleón-Pradas, J.L. Gómez-Ribelles, Plasma-induced polymerisation of hydrophilic coatings onto macroporous hydrophobic scaffolds, Polymer (Guildf). 48 (2007) 2071–2078.

[23] Á. Serrano-Aroca, M. Monleón-Pradas, J.L. Gómez-Ribelles, J. Rault, Thermal analysis of water in reinforced plasma-polymerised poly(2-hydroxyethyl acrylate) hydrogels, Eur. Polym. J. 72 (2015) 523–534.

[24] Á. Serrano-Aroca, J.L. Gómez-Ribelles, M. Monleón-Pradas, A. Vidaurre-Garayo, J. Suay-Antón, Characterisation of macroporous poly(methyl methacrylate) coated with plasma-polymerised poly(2-hydroxyethyl acrylate),

Eur. Polym. J. 43 (2007) 4552–4564.

[25] Á. Serrano-Aroca, J.F. Ruiz-Pividal, M. Llorens-Gámez, Enhancement of water diffusion and compression performance of crosslinked alginate with a minuscule amount of graphene oxide, Sci. Rep. 7 (2017) 11684. doi:10.1038/s41598-017-10260-x.

[26] Á. Serrano-Aroca, S. Deb, Synthesis of irregular graphene oxide tubes using green chemistry and their potential use as reinforcement materials for biomedical applications, PLoS One. 12 (2017) e0185235. doi:10.1371/journal.pone.0185235.

[27] F. Sánchez-Correa, C. Vidaurre-Agut, A. Serrano-Aroca, A.J. Campillo-Fernández, Poly(2-hydroxyethyl acrylate) hydrogels reinforced with graphene oxide: Remarkable improvement of water diffusion and mechanical properties, J. Appl. Polym. Sci. (2018) 46158. doi:10.1002/app.46158.

[28] S. Faghihi, M. Gheysour, A. Karimi, R. Salarian, Fabrication and mechanical characterization of graphene oxide-reinforced poly (acrylic acid)/gelatin composite hydrogels, J. Appl. Phys. 115 (2014).

[29] X. Rui-Hong, R. Peng-Gang, H. Jian, R. Fang, R. Lian-Zhen, S. Zhen-Feng, Preparation and properties of graphene oxide-regenerated cellulose/polyvinyl alcohol hydrogel with pH-sensitive behavior, Carbohydr. Polym. 138 (2016) 222–228.

[30] J. Zhao, L. Liu, F. Li, Graphene Oxide: Physics and Applications, Springer, 2014.

[31] J. Wang, C. Liu, Y. Shuai, X. Cui, L. Nie, Controlled release of anticancer drug using graphene oxide as a drug-binding effector in konjac glucomannan/sodium

alginate hydrogels, Colloids Surfaces B Biointerfaces. 113 (2014) 223–229.

[32] X. Yang, Y. Wang, X. Huang, Y. Ma, Y. Huang, R. Yang, H. Duan, Y. Chen, Multi-functionalized graphene oxide based anticancer drug-carrier with dual-targeting function and pH-sensitivity, J. Mater. Chem. 21 (2011) 3448–3454.

[33] W. Shao, X. Liu, H. Min, G. Dong, Q. Feng, S. Zuo, Preparation, characterization, and antibacterial activity of silver nanoparticle-decorated graphene oxide nanocomposite., ACS Appl. Mater. Interfaces. 7 (2015) 6966–73.

[34] S. Jin, D. Xu, N. Zhou, J. Yuan, J. Shen, Antibacterial and anticoagulation properties of polyethylene/geneO-MPC nanocomposites, J. Appl. Polym. Sci. 129 (2013) 884–891.

[35] M. Ionita, M.A. Pandele, H. Iovu, Sodium alginate/graphene oxide composite films with enhanced thermal and mechanical properties, Carbohydr. Polym. 94 (2013) 339–344.

[36] Y. He, N. Zhang, Q. Gong, H. Qiu, W. Wang, Y. Liu, J. Gao, Alginate/graphene oxide fibers with enhanced mechanical strength prepared by wet spinning, Carbohydr. Polym. 88 (2012) 1100–1108.

[37] M. Yadav, K.Y. Rhee, S.J. Park, Synthesis and characterization of graphene oxide/carboxymethylcellulose/alginate composite blend films., Carbohydr. Polym. 110 (2014) 18–25.

[38] J. Fan, Z. Shi, M. Lian, H. Li, J. Yin, Mechanically strong graphene oxide/sodium alginate/polyacrylamide nanocomposite hydrogel with improved dye adsorption capacity, J. Mater. Chem. A. 1 (2013) 7433.

[39] M. Park, B.H. Kim, S. Kim, D.S. Han, G. Kim, K.R. Lee, Improved binding between copper and carbon nanotubes in a composite using oxygen-containing functional groups, Carbon N. Y. 49 (2011) 811–818.

[40] S. Park, K.-S. Lee, G. Bozoklu, W. Cai, S.T. Nguyen, R.S. Ruoff, Graphene oxide papers modified by divalent ions-enhancing mechanical properties via chemical cross-linking., ACS Nano. 2 (2008) 572–578.

[41] H. Bai, C. Li, X. Wang, G. Shi, On the Gelation of Graphene Oxide, J. Phys. Chem. C. 115 (2011) 5545–5551. doi:10.1021/jp1120299.

[42] Á. Serrano-Aroca, S. Deb, Synthesis of irregular graphene oxide tubes using green chemistry and their potential use as reinforcement materials for biomedical applications, PLoS One. 12 (2017). doi:10.1371/journal.pone.0185235.

[43] J. Crank, The mathematics of diffusion second edition, Oxford University Press, 1975.

[44] A. Jejurikar, G. Lawrie, D. Martin, L. Grøndahl, A novel strategy for preparing mechanically robust ionically cross-linked alginate hydrogels., Biomed. Mater. 6 (2011) 25010. doi:10.1088/1748-6041/6/2/025010.

[45] K. Vilcinskas, J. Zlopasa, K.M.B. Jansen, F.M. Mulder, S.J. Picken, G.J.M. Koper, Water Sorption and Diffusion in (Reduced) Graphene Oxide-Alginate Biopolymer Nanocomposites, Macromol. Mater. Eng. 301 (2016) 1049–1063.

[46] M. Ma, G. Tocci, A. Michaelides, G. Aeppli, Fast diffusion of water nanodroplets on graphene, Nat Mater. 15 (2016) 66–71.

[47] P. Sun, H. Liu, K. Wang, M. Zhong, D. Wu, H. Zhu, Ultrafast liquid water

transport through graphene-based nanochannels measured by isotope labelling, Chem. Commun. 51 (2015) 3251–3254.

[48] J.K. Holt, Fast Mass Transport Through Sub-2-Nanometer Carbon Nanotubes, Science (80-.). 312 (2006) 1034–1037.

[49] M. Majumder, N. Chopra, R. Andrews, B.J. Hinds, Nanoscale hydrodynamics: enhanced flow in carbon nanotubes., Nature. 438 (2005) 44.

[50] D.W. Boukhvalov, M.I. Katsnelson, Y.W. Son, Origin of anomalous water permeation through graphene oxide membrane, Nano Lett. 13 (2013) 3930–3935.

[51] R.R. Nair, H.A. Wu, P.N. Jayaram, I. V. Grigorieva, A.K. Geim, Unimpeded Permeation of Water Through Helium-Leak-Tight Graphene-Based Membranes, Science (80-.). 335 (2012) 442–444.

[52] F.M. Fowkes, Attractive forces at interfaces, Ind. Eng. Chem. 56 (1964) 40–52. doi:10.1021/ie50660a008.

[53] D.K. Owens, R.C. Wendt, Estimation of the surface free energy of polymers, J. Appl. Polym. Sci. 13 (1969) 1741–1747. doi:10.1002/app.1969.070130815.

[54] R.J. Good, Contact angle, wetting, and adhesion: a critical review, J. Adhes. Sci. Technol. 6 (1992) 1269–1302. doi:10.1163/156856192X00629.

[55] C. Sartori, D.S. Finch, B. Ralph, K. Gilding, Determination of the cation content of alginate thin films by FTi.r. spectroscopy, Polymer (Guildf). 38 (1997) 43–51. doi:10.1016/S0032-3861(96)00458-2.

[56] K. Nakamoto, Infrared and Raman Spectra of Inorganic and Coordination Compounds, Theory and Applications in Inorganic Chemistry, John Wiley &

Sons, 2008. https://books.google.com/books?id=9t3h8pVgnyQC&pgis=1 (accessed October 4, 2016).

Highlights

- New composites with enhanced mechanical, thermal, wettability and water diffusion
- Green and sustainable synthesis without consuming thermal or sonic energy
- Clean and facile technology that exhibits affordable large-scale production
- Crosslinking of graphene oxide nanosheets by coordination chemistry
- Improvement of several alginate's physical properties at the same time

Graphical abstract